THE JOURNAL OF BIOLOGICAL CHEMISTRY
Vol. 279, No. 53, Issue of December 31, pp. 55308–55314, 2004
Printed in U.S.A.

Direct Measurement of the Thermodynamic Parameters of Amyloid Formation by Isothermal Titration Calorimetry*

Received for publication, August 23, 2004, and in revised form, October 4, 2004
Published, JBC Papers in Press, October 19, 2004, DOI 10.1074/jbc.M409677200

József Kardos‡§¶‖, Kaori Yamamoto‡¶, Kazuhiro Hasegawa, Hironobu Naiki**, and Yuji Goto‡ ‡‡**

*From the ‡Institute for Protein Research, Osaka University and CREST, Japan Science and Technology Agency, Yamadaoka 3-2, Suita, Osaka 565-0871, Japan, the §Department of Biochemistry, Eötvös University, Pázmány sétány 1/C, Budapest, 1117, Hungary, and the **Faculty of Medical Sciences, University of Fukui and CREST, Japan Science and Technology Agency, Matsuoka, Fukui 910-1193, Japan*

Amyloid fibril deposition is associated with over 20 degenerative diseases, including Alzheimer's, Parkinson's, and prion diseases. Although research over the last few years has revealed the morphology and structural features of the amyloid form, knowledge about the thermodynamics of amyloid formation is limited. Here, we report for the first time a direct thermodynamic study of amyloid formation using isothermal titration calorimetry. β_2-Microglobulin, a protein responsible for dialysis-related amyloidosis, was used for extending amyloid fibrils in a seed-controlled reaction in the cell of the calorimeter. We investigated the enthalpy and heat capacity changes of the reaction, where the monomeric, acid-denatured molecules adopt an ordered, cross-β-sheet structure in the rigid amyloid fibrils. Despite the dramatic difference in morphology, β_2-microglobulin exhibited a similar heat capacity change upon amyloid formation to that of the folding to the native globular state, whereas the enthalpy change of the reaction proved to be markedly lower. In comparison with the native state, the results outline the important structural features of the amyloid fibrils: a similar extent of surface burial even with the supramolecular architecture of amyloid fibrils, a lower level of internal packing, and the possible presence of unfavorable side chain contributions.

Amyloid fibril deposition of different proteins is manifested in over 20 degenerative disorders including Alzheimer's disease, transmissible spongiform encephalopathies, and dialysis-related amyloidosis (1–3). The increasing wealth of information accumulated in recent years has proven that the ability to form amyloid structures is a general property of the polypeptide chains. A large number of proteins and peptides have been shown to be capable of polymerization into amyloid fibrils *in vitro* under appropriate conditions, such as low pH, high temperature, or moderate concentrations of salts or co-solvents (1, 4–7). Amyloid fibrils are characterized by a cross-β-structure where β-strands are perpendicularly oriented to the axis of the fibrils (8). The morphology and structure of the amyloid form have been widely studied using electron microscopy, atomic force microscopy, x-ray diffraction, solid state NMR, and several spectroscopic methods (1, 2, 4–10). Kinetic studies showed that the amyloid formation is a nucleation-dependent complex reaction (see the detailed review of Stefani and Dobson (5)).

Despite the numerous studies on protein misfolding and amyloidosis, knowledge on the thermodynamics of amyloid formation is limited. Several studies have reported the structural and thermodynamic requirements of fibril formation from the side of the amyloidogenic precursor, showing the role of the stability of the native state in the amyloidogenicity or the importance of the accumulation of intermediate states (11–13). Recent studies have revealed the importance of general physicochemical characteristics of the polypeptide chain, such as the hydrophobicity, secondary structure propensity, and overall charge in the amyloid formation (14, 15).

The direct thermodynamic characterization of the unfolding and stability of globular proteins is well established by physicochemical techniques, especially by differential scanning calorimetry (DSC)[1] (16, 17). However, it has been difficult to describe the thermodynamic properties of the amyloid form with these techniques because of the high stability of amyloid fibrils, the inhomogeneity of the aggregated samples, the irreversibility of the transitions, and problems with reproducibility. The difficulties are clearly demonstrated by the fact that, in the PubMed data base, of over 6000 hits searching for "differential scanning calorimetry," only two dozen are related to amyloidosis. These works either investigated the unfolding and stability of the monomer forms of amyloidogenic proteins or amyloidogenic variants (18–21) or sign the formation of aggregates/amyloid fibrils from the irreversible nature and unusual shape of the thermal unfolding profile (22). No results were reported on the direct measurement of the thermodynamic properties of amyloid extension. However, we believe that the amyloid fibril formation is a reversible thermodynamic process, unless the extensive association of fibrils causes an irreversible aggregation.

Isothermal titration calorimetry (ITC) is a delicate method for the study of the heat effect of ligand binding to proteins or the study of protein association (23, 24). Related to the problem of amyloid formation, Kim *et al.* (25) studied the binding of an amyloid-specific dye, Congo Red to an immunoglobulin light

* This work was supported in part by Grants-in-aid for Scientific Research 40153770 and 13480219 from the Japanese Ministry of Education, Culture, Sports, Science and Technology on Priority Areas and Scientific Research (B). The costs of publication of this article were defrayed in part by the payment of page charges. This article must therefore be hereby marked "*advertisement*" in accordance with 18 U.S.C. Section 1734 solely to indicate this fact.

¶ These authors equally contributed to this work.
‖ Supported by the Japan Society for the Promotion of Science.
‡‡ To whom correspondence should be addressed: Institute for Protein Research, Osaka University, Yamadaoka 3-2, Suita, Osaka 565-0871, Japan. Tel.: 81-6-6879-8614; Fax: 81-6-6879-8616; E-mail: ygoto@protein.osaka-u.ac.jp.

[1] The abbreviations used are: DSC, differential scanning calorimetry; ITC, isothermal titration calorimetry; β2m, β_2-microglobulin; ThT, thioflavin T.

chain variable domain inducing partial unfolding into the amyloidogenic precursor state. Terzi *et al.* (26) studied the binding of Alzheimer β-amyloid peptide 1–40 to lipid membranes and the random coil-to-β-sheet transition of the β-amyloid 25–35 fragment (27). There is great demand to explore using thermodynamic approaches the role of the different interactions such as hydration, nonpolar interactions, hydrogen bonds, and salt bridges in the formation and stability of the amyloid fibrils.

Here, we introduce a novel method for the direct thermodynamic study of amyloid formation by ITC. As a model system, we selected the amyloid fibril formation of β_2-microglobulin (β2m), a protein responsible for dialysis-related amyloidosis, a common and serious complication in patients receiving hemodialysis for more than 10 years (3, 28). β2m is the light chain of the type I major histocompatibility complex and also appears in a monomeric form in the blood. In the native state, β2m adopts a typical immunoglobulin fold consisting of seven β-strands organized into two β-sheets connected by a single disulfide bridge (see Fig. 1*A*). The mechanism and the important factors of the *in vivo* amyloid formation of β2m are not yet well understood. We investigated the enthalpy (ΔH) and heat capacity (ΔC_p) changes of the seed-dependent extension of β2m amyloid fibrils under acidic conditions and compared them with those of the folding of the native β2m.

EXPERIMENTAL PROCEDURES

Protein, Amyloid Fibrils, and Seeds—Recombinant β2m was expressed and purified as described previously (29). The protein concentration was determined using an extinction coefficient of $1.91 \times 10^4\ M^{-1}\ cm^{-1}$ at 280 nm. Amyloid fibril formation of β2m was carried out by the seed-dependent fibril extension method (30, 31). The reaction was monitored by fluorometric analysis with ThT (31). Seeds (*i.e.* fragmented fibrils) were prepared by sonication of 200-μl aliquots from a 0.3 mg/ml fibril stock solution using a Microson sonicator (Misonix, Farmingdale, NY) at intensity level 2, forty 1-s pulses on ice.

Estimation of the Monomeric β2m Concentration in the Fibril Solution—β2m fibrils were grown in reaction mixtures containing 0.1 mg/ml monomers and 30 μg/ml seeds at 10, 25, and 37 °C, in 50 mM sodium citrate, 100 mM NaCl (pH 2.5) buffer. The samples were incubated for 24 h, to reach fibril-monomer equilibrium. To separate the monomers from the fibrils, the samples were spun down at 40,000 rpm at the same temperatures as the extension in a CS 120GX ultracentrifuge (Hitachi, Tokyo, Japan) for 30 min. In the case of studying solutions of low protein concentration adsorption of the protein to the surface of the vials, tubes may decrease the free protein concentration significantly and thus alter the results. To avoid the loss of the monomeric β2m component from the equilibrium fibril-monomer solution during the centrifugation through adsorption by the tube walls, the extension reactions were carried out in the centrifuge tubes providing sufficient monomers (0.1 mg/ml) at the beginning of the reactions to saturate the possible adsorption effect. The centrifugal force ($60{,}000 \times g$) used is not able to sediment the monomer β2m. The monomer β2m concentrations were determined by enzyme-linked immunosorbent assay using a commercial immunoassay kit (Glazyme β_2-microglobulin EIA test; Wako, Osaka, Japan). After separation of the monomer component, Tween 20 was added at a final concentration of 0.05% (v/v) to exclude any protein adsorption on the labware. Then 2-, 4-, 6-, and 10-fold dilution series of the samples were assayed using standard β2m solutions of 0, 50, 100, and 200 ng/ml as references. The assay presented a sensitive and quasi-linear concentration dependence in the 0–200 ng/ml range.

CD Spectroscopy—Thermal unfolding of β2m was followed using a J-720 spectropolarimeter (Jasco, Tokyo, Japan) equipped with a Peltier cell holder. A quartz cell with a path length of 5 mm was used. The protein concentration was 0.06 mg/ml in 20 mM sodium citrate or 20 mM sodium phosphate buffer depending on the pH. The unfolding was followed at 220 nm using a heating rate of 30 °C/h.

Calorimetry—DSC experiments were carried out with a VP-DSC instrument (MicroCal, Northampton, MA). The protein concentration was 0.3 mg/ml in 50 mM sodium phosphate buffer (pH 7.0) containing 100 mM NaCl. The thermal unfolding curves were analyzed using MicroCal Origin 7.0 software.

ITC measurements to determine the enthalpy changes of the seed-dependent extension reaction of β2m fibrils were performed with a Microcal VP-ITC instrument. In one experimental set-up, the cell was filled with monomer β2m, and the syringe was filled with β2m amyloid seed solution. The reaction was started with a single injection of seeds into the cell at a final seed concentration of 15 μg/ml. The same buffer (50 mM sodium citrate at pH 2.5 containing 100 mM NaCl, pH 2.5) was used in both the syringe and the cell.

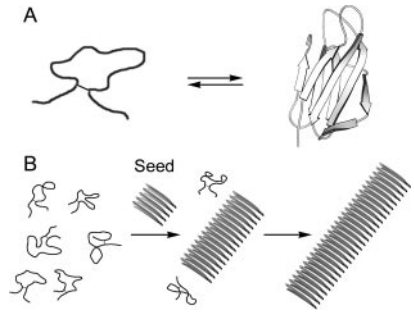

FIG. 1. **Representation of the alternative folding processes of β2m.** *A*, folding of the native globular state. *B*, amyloid fibril extension in which the acid-denatured β2m molecules extend the seeds taking up the ordered cross-β-sheet structure.

In an inverse experimental set-up, the calorimeter cell was filled with a seed solution of 30 μg/ml. The extension reaction was initiated by the injection of monomer β2m into the cell. The concentration of monomer in the syringe was 0.57, 0.7, or 1.0 mg/ml. Experiments with five 10-μl injections were performed. 50 mM sodium citrate buffer (pH 2.5) containing 100 mM NaCl was used in the cell. To avoid the spontaneous aggregation of β2m, no salt was used in the syringe. To remove any contamination of aggregated material, prior to the measurements all of the monomer samples in both experimental set-ups were spun down at 40,000 rpm for 30 min.

Electron Microscopy—Electron micrographs of amyloid fibrils were taken as described before (29).

RESULTS

Thermal Unfolding of the Native State—Amyloid fibril formation of β2m is an association-induced misfolding process producing rigid amyloid fibrils with an ordered structure (Fig. 1). To discover the distinct thermodynamic properties in the amyloid state, it is important to compare the parameters of the amyloid state with those of the native state. The properties focused on are the enthalpy (ΔH) and heat capacity (ΔC_p) changes of fibril formation and their contributions to the free energy change (ΔG).

We first carried out the heat denaturation of the native state followed by CD at various pH values (Fig. 2*A*). β2m exhibited cooperative unfolding transition in the pH range 3.7–8.0. The advantage of this technique was that at a protein concentration as low as 0.06 mg/ml, the thermal unfolding of β2m was completely reversible in the pH range 5–8 and fairly reversible at $pH < 5$. At 37 °C, β2m is marginally stable or unstable at $pH < 5$, with the unfolding transition underway, so that the denatured state is significantly populated (Fig. 2*A*).

Although the presence of intermediates in the thermal unfolding process cannot be excluded, a two-state model provided a good fitting, valuable for comparison with the amyloid formation process. The van't Hoff enthalpy changes (ΔH_{vH}) of the unfolding transitions were calculated. The reversibility of all the samples was checked by a second scan. In the case of partly reversible transitions in the lower pH range, ΔH_{vH} and the melting temperatures (T_m) of the second scans were found to be similar to those of the first scans within 10% and 0.5 °C, respectively. ΔH_{vH} as a function of T_m showed a linear dependence (Fig. 2*B*). The slope of the fitted line provides ΔC_p upon unfolding, which was found to be $5.6 \pm 0.4\ kJ \cdot mol^{-1} \cdot K^{-1}$.

To check the validity of the two-state model, we carried out a DSC measurement using 0.3 mg/ml β2m at pH 7.0 (Fig. 2*C*). The two-state fitting was in good agreement with the observed calorimetric curve. The calorimetric and van't Hoff enthalpy changes with a ratio of 0.98 are similar to ΔH_{vH} obtained from

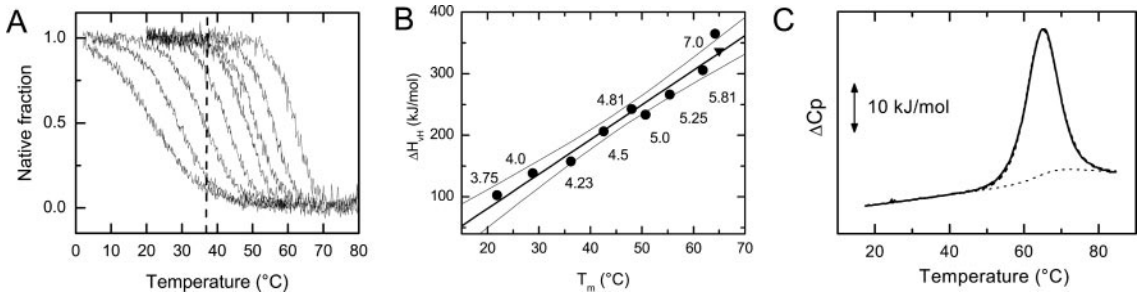

FIG. 2. **Thermal denaturation of the native state of β2m.** *A*, thermal denaturation of β2m as a function of pH followed by CD spectroscopy. The pH value was varied in the experiments from the *left* unfolding curve to the *right* as follows: 3.75, 4.0, 4.23, 4.5, 4.81, 5.0, 5.25, and 5.8. The *dashed line* shows 37 °C. *B*, ΔH as a function of T_m and fitting for ΔC_p. The 95% confidence limits are presented by *thin lines*. ●, results from CD; ▼, result of DSC at pH 7.0. *C*, *solid line*, DSC melting profile of β2m in 50 mM sodium phosphate, 100 mM NaCl at pH 7.0; *dashed line*, two-state fitting; *dotted line*, base line.

the CD measurements (Fig. 2*B*). The reversibility determined from the calorimetric enthalpy change of the second scan was 85%. It was difficult to determine ΔC_p directly from the DSC melting profile because of the slightly declining heat capacity curve after the unfolding transition, although a rough estimation of ΔC_p at the melting temperature presented a similar value of 5.5 ± 1 kJ·mol^{-1}·K^{-1}. In Table I, the main parameters of the native β2m at pH 7.0 are presented at three different temperatures.

Monomer-Fibril Equilibrium in the Solution—To measure the heat effects of fibril formation, we adapted the seed-dependent fibril extension method of Naiki *et al.* (30, 31) to ITC. At pH 2.5, monomeric β2m is disordered with a lack of significant amide-proton protection (32) and shows no thermal unfolding transition in the CD or DSC measurements (data not shown). The pH-dependent unfolding experiments by CD (Fig. 2, *A* and *B*) also verify this, showing that decreasing the pH to 3.75, monomeric β2m becomes unfolded even at room temperature. In the seed-dependent extension reaction at pH 2.5, fibrils are extended via the consecutive association of unfolded monomeric β2m onto the ends of the fibrils without a change in the number of fibrils (33). The concentration of fibrils is determined by the number of seeds added to the solution to start the reaction (Fig. 1*B*). Although it is difficult to determine the exact number of seeds and thus the starting fibril/monomer ratio in the solution, under the conditions used in this study monomers extended the seeds resulting in 50-nm-long to 1-μm-long fibrils as also can be seen in Fig. 3. If the β2m monomer solution was free from any aggregated material, no spontaneous fibril formation occurred during the time course of the experiment.

The seed-dependent extension of β2m fibrils has been validated experimentally by the following model (33, 34),

$$[P] + [M] \underset{k_{-1}}{\overset{k_1}{\rightleftharpoons}} [P] \qquad \text{(Eq. 1)}$$

where [P] is the concentration of seed fibrils, [M] is the concentration of monomer β2m, and k_1 and k_{-1} are the apparent rate constants for polymerization and depolymerization, respectively. In the equilibrium of association and dissociation.

$$k_1[M][P] = k_{-1}[P] \qquad \text{(Eq. 2)}$$

As we can see, the equilibrium will be independent of [P] in this type of reaction, where the concentration of the fibrils (*i.e.* the concentration of the extendable fibril ends) does not change. We obtain the equilibrium monomer concentration (critical monomer concentration) $[M]_e$ as follows,

$$[M]_e = k_{-1}/k_1 = 1/K \qquad \text{(Eq. 3)}$$

where K is the equilibrium association constant. By determining $[M]_e$, we can obtain K. Then we can calculate the apparent free energy change (ΔG_{app}) of the extension reaction, *i.e.* ΔG_{app} upon the folding from the acid-denatured monomeric state into the amyloid state.

To adapt the seed-dependent fibril extension to ITC, several factors had to be taken into account such as base-line stability, sensitivity of the instrument, response time of the instrument, and equilibration time of the system prior to the measurement. Among them, the evaluation of the $[M]_e$ value is essential for the set-up of the extension reaction in the calorimeter; the concentration of seeds in the monomer unit must be higher than $[M]_e$. Otherwise, the seeds will depolymerize to monomers. To determine $[M]_e$, extension reactions at 0.1 mg/ml β2m were carried out in the centrifuge tubes for 24 h at 37, 25, and 10 °C. Then the fibrils were removed from the solution by ultracentrifugation. The monomer concentrations of the supernatants, $[M]_e$, which were too low to be detected by absorption, were determined quantitatively by immunoassay to be 84 nM at 10 °C, and the value decreased slightly with an increase in temperature (Table I). Although the ultracentrifugation procedure of removing the fibrils theoretically may leave small nonfibrillar oligomers in the solution, such oligomers supposed to be not involved in the seed-induced fibril extension reaction of β2m, where monomers extend the fibril ends (30, 31, 33, 34). Moreover, small oligomers could not be detected by analytical ultracentrifugation of β2m solutions at pH 2.5.[2] The presence of such small oligomer contamination would mean that the equilibrium monomer concentration is even smaller than the value determined by the immunoassay. 30 μg/ml (~2.5 μM β2m monomers) seed concentration, which is much higher than $[M]_e$, was chosen for the ITC measurements of titrating the seed fibrils with monomers. We expect that our experimental conditions provide enough protein to reach the monomer-fibril equilibrium and to assure that all the injected monomers will be converted to fibrils in a rapid reaction.

Fibril Extension Followed by ITC—The reaction started promptly with the addition of monomers to the seed solution or vice versa on injection of the seeds into the monomer solution. The electron microscopy image of β2m fibrils formed in the ITC cell showed typical straight amyloid fibrils, confirming the seed-dependent fibril extension (Fig. 3). Fig. 4*A* shows the extension reaction monitored by heat and its references when 75 μl of seed solution was injected at a final concentration of 15 μg/ml into the cell containing 0.1 mg/ml of monomer β2m solution. The areas of the peaks represent the ΔH values of the reactions. Both in the syringe and in the cell, 50 mM sodium citrate buffer (pH 2.5) containing 100 mM NaCl

[2] J. Kardos, M. Sakai, and Y. Goto, unpublished results.

TABLE I
Unfolding thermodynamic parameters of the native monomeric β2m and of the amyloid form

Temperature	ΔH		ΔG (native)	ΔG_{app} (amyloid)	$[M]_e$ (amyloid)	$-T\Delta S$[a]		ΔC_p[b]	
	Native	Amyloid				Native	Amyloid	Native	Amyloid
	kJ·mol⁻¹		*kJ·mol⁻¹*	*kJ·mol⁻¹*	*nM*	*kJ·mol⁻¹*		*kJ·mol⁻¹·K⁻¹*	
10 °C	23.2 ± 5	−14.2 ± 3	25.8 ± 1.8	38.4 ± 0.3	84 ± 10	2.6 ± 3	52.6 ± 3		
25 °C	107.2 ± 5	57.6 ± 2	23.9 ± 0.9	41.7 ± 0.2	50 ± 3	−83.3 ± 4	−15.9 ± 2	5.6 ± 0.4	4.78 ± 0.21
37 °C	174.7 ± 8	124 ± 3	19.1 ± 0.4	43.9 ± 0.2	41 ± 3	−155.6 ± 6.5	−80 ± 3		

[a] Calculated by $\Delta G = \Delta H - T\Delta S$; for the amyloid form, the apparent ΔG values were used as an estimation.
[b] The common values for different temperatures were obtained.

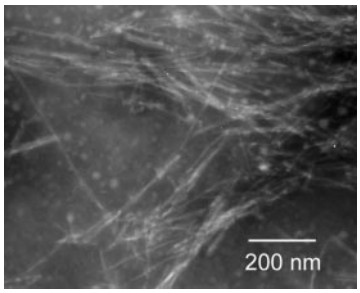

FIG. 3. **Electron microscopy image of β2m fibrils formed in the calorimeter cell.** The final protein concentration in the calorimeter was 10 μM.

was used. The net ΔH upon the amyloid formation was calculated as follows,

$$\Delta H_{u\to f} = \Delta H_{SM} - \Delta H_{SB} - \Delta H_{BM} + \Delta H_{BB} \quad \text{(Eq. 4)}$$

where SM, SB, BM, and BB are measurements of injections of seeds into the monomer solution (extension reaction), seeds into buffer, buffer into the monomer solution, and buffer into buffer, respectively, and normalized for the molar amount of associated monomers. The buffer to buffer effect is included in the subtracted ΔH_{SB} and ΔH_{BM}, so that the net effect is given by the addition of ΔH_{BB}. The three references proved to be similar to one another and exhibited only ~3% of $\Delta H_{u\to f}$. The enthalpy change of the β2m amyloid fibril extension as an average of three measurements at 37 °C was −124 ± 3 kJ/mol. Fig. 4*B* represents ΔH of the reaction as a function of time by the integration of the ΔP peak of the reaction shown in Fig. 4*A*, corrected by the references. This represents the kinetics of the reaction via the enthalpy production, indicating the high accuracy and low noise of the measurement even without smoothing of the data. $\Delta H(t)$ could be fitted well by a single exponential decay with a time constant of 33 min. The slight deviation of the observed curve from the fitted curve may arise from: 1) the relatively slow response time (2–3 min) of the instrument; 2) a decreasing number of seeds (extendable fibril ends) in the long experiment by the aggregation of fibrils; and 3) the extension is not purely a single exponential for unknown reasons. Other spectroscopic methods are probably unable to point out such differences because of the larger fluctuations in the experimental data.

The time course of the extension reaction was followed by ThT binding as a complementary method using the same seed and monomer concentrations (Fig. 4*C*). The seed and monomer solutions were preincubated at 37 °C for 1 h, the approximate time needed for the equilibration of the ITC before starting the reaction. After starting the reaction, the ThT fluorescence intensity reached a maximum faster than ΔH monitored by ITC. The time constant on the basis of a single exponential decay was 12.5 min fitted for the first 40 min of the reaction (Fig. 4*C*). The reason might be the different sensitivity and selectivity for aggregates of the two methods. In the case of the ThT assay, a declination of the fluorescence intensity is often visible after reaching its maximum (35, 36), suggesting that the clustering of preformed amyloid fibrils suppresses the ThT binding. On the other hand, ITC may be able to show a process hardly detectable by ThT binding. For example, it is likely that the clustering of preformed amyloid fibrils contributes to the observed slow heat effects. Although the difference in the kinetics monitored by ITC and ThT needs further investigation, it is clear that the kinetics of amyloid fibril formation can be monitored by ITC.

Temperature Dependence of ΔH of Fibril Extension—The extension reaction was carried out at eight different temperatures in the 26–50 °C range using a reverse experimental setup, *i.e.* injection of monomers into the seed solution of the calorimeter cell. In these experiments, no salt was used in the concentrated monomer solution of the syringe to avoid aggregation. This required careful reference subtraction because of the heat effect of salt dilution. The advantage of this technique was that we could inject a small amount of β2m monomer solution repeatedly, assuring fast and complete reactions at a temperature as low as 26 °C where the reaction is slow. Moreover, with no salt in the syringe we avoided the aggregation of stock monomers at higher temperatures such as 50 °C.

ITC raw data on injecting five 10-μl aliquots of 0.57 mg/ml β2m monomer solution into the ITC cell filled with 30 μg/ml seed solution at 30 °C showed repeated heat effects (*i.e.* negative spikes) caused by the fibril extension (Fig. 5*A*). To avoid the usual uncertainty of the first injection, a small, 2-μl aliquot was injected at the beginning of the experiment. Fig. 5*B* presents the enthalpy changes of the extension reactions and their references at various temperatures. The $\Delta H_{u\to f}$ values corrected with the references and normalized for molar associated monomers indicated a linear temperature dependence with a slope of −4.78 kJ·mol^{-1}·K^{-1} (Fig. 5*C* and Table I). It is noted in Table I that, the thermodynamic parameters of the native and amyloid states are indicated in the direction of unfolding and dissociation following the usual practice in protein stability and unfolding studies (16, 17, 37, 39–41). This parameter (−4.78 kJ·mol^{-1}·K^{-1}) is the heat capacity change (ΔC_p) upon formation of the amyloid structure from the acid-denatured monomer. The agreement of the $\Delta H_{u\to f}$ value at 37 °C obtained by injecting the monomers (−119.2 ± 4 kJ/mol) with that by injecting the seeds (−124 ± 3 kJ/mol) substantiates the validity of the experiments.

DISCUSSION

ΔC_p, Suggesting a Similar Overall Surface Burial—It has been known that the heat capacity change upon protein unfolding is primarily given by the hydration of the polar and apolar groups (~95%) and to a much lesser extent by disruption of the internal noncovalent interactions such as van der Waals' interactions, H-bonds, ionic interactions, etc. (17, 37). An empirical function reliably predicts ΔC_p associated with the unfolding transitions of native globular proteins in terms of the change in the accessible polar and apolar surface areas and in the total buried surface area (ΔASA_{apol}, ΔASA_{pol}, and ΔBSA_{tot}, respectively),

$$\Delta C_p = \Delta C_{p,hydr} + \Delta C_{p,noncov} = a\cdot\Delta ASA_{apol} - b\cdot\Delta ASA_{pol} + c\cdot\Delta BSA_{tot} \quad \text{(Eq. 5)}$$

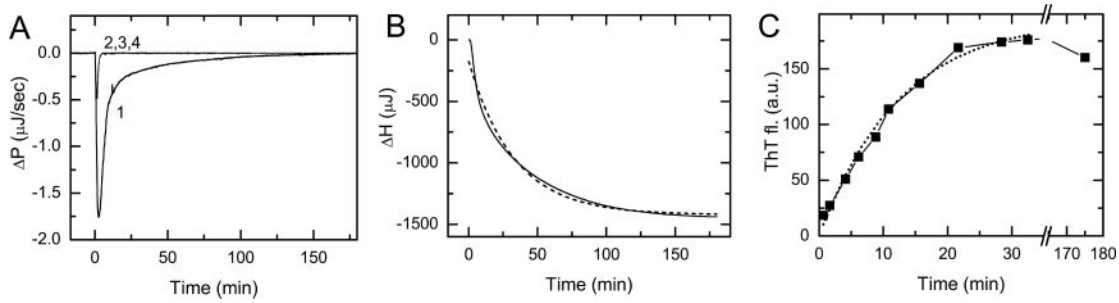

FIG. 4. **Kinetics of β2m fibril extension monitored by heat.** *A*, heat effect on the extension of β2m fibrils followed by the injection of seeds at a final concentration of 15 μg/ml into 0.1 mg/ml monomer β2m solution of the ITC cell at 37 °C (*line 1*). Overlapping *thin lines* represent the reference measurements as buffer to buffer (*line 2*), buffer to monomers (*line 3*), and seeds to buffer solution (*line 4*). *B*, enthalpy change of the extension reaction as a function of time (*solid line*) and an exponential fitting (*dashed line*). *C*, fibril extension reaction of β2m under the same experimental conditions followed by ThT fluorescence. *Dotted line*, fitting with exponential decay.

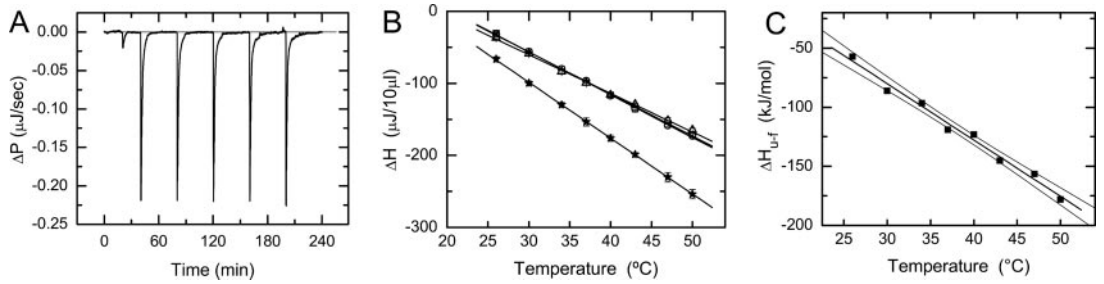

FIG. 5. **Temperature dependence of the heat effects of fibril extension.** *A*, typical ITC data on injecting five 10-μl aliquots of 0.57 mg/ml β2m monomer solution into a 30 μg/ml seed solution at 30 °C. *B*, enthalpy changes of the extension reaction and reference measurements carried out at different temperatures. The averages of five injections are shown. ■, buffer to buffer injection; ●, buffer injected to the seed solution; △, monomers injected to buffer; ⋆, fibril formation by injecting monomers to the seed solution. The *error bars* are presented. *C*, molar enthalpy change of the extension reaction as a function of temperature. The slope of the *fitted line* provides ΔC_p upon amyloid formation. The 95% confidence bands are also shown.

where *a*, *b*, and *c* are empirical parameters for the hydrations of apolar and polar groups and for the internal noncovalent interactions, respectively (adopted from Ref. 37).

Compared with the native monomeric state, we may expect a higher extent of surface burial upon the association of β2m molecules in amyloid fibrils because of their supramolecular architecture; the proportion of the buried surface increases with an increase in the size of the folded state. To estimate the surface burial and ΔC_p upon amyloid formation, we carried out model calculations taking into account the rod-like morphology and characteristic dimensions of amyloid fibrils obtained from atomic force microscopy studies (36, 38) and assuming a native-like packing density and ratio of apolar and polar surface burial (from Protein Data Bank code 1hsb). Based on Equation 5, calculations for protofibrils with a diameter of 5 nm and fibrils consisting of two or three associated protofibrils resulted in an ~1.5–2.0 times higher ΔC_p. However, the experimental results have disproved these calculations, showing a ΔC_p value similar to that on the unfolding of the native β2m (Table I). Considering that ΔC_p is mainly derived from the hydration, *i.e.* from the change of the solvent-accessible surfaces, a similar ΔC_p of the unfolding of the native and amyloid states of β2m (5.6 *versus* 4.78 $kJ \cdot mol^{-1} \cdot K^{-1}$; Table I) indicates a similar overall burial of surface in the two forms. The supramolecular structure of amyloid fibrils suggests that this unexpectedly low surface burial might be realized through the existence of a variety of cavities accessible for bulk water located inside and between the protofilaments constituting the amyloid fibrils. Moreover, it is likely that the surface of β2m fibrils is not as "smooth" as that of the native protein.

The native globular structure of β2m is a result of protein evolution with optimal packing and burial of apolar and polar side chains. On the contrary, the amyloid structure of the same polypeptide chain is determined by the H-bonded and extended intermolecular β-sheet architecture of the peptide backbones; consequently, the side chain interactions and packing bear a secondary role in the structure (42). Various poly-amino acids can form amyloid fibrils. Studies with x-ray fiber diffraction of amyloid fibrils made of poly-amino acids indicate that while the distance between β-strands is constant (*i.e.* 4.7 Å), the distance between the β-sheet layers varies depending on the bulkiness of the side chains (42). Because the natural amyloidogenic proteins are made of various amino acid residues, it is unlikely that tight packing of the side chain, as present in the interior of native proteins, is achieved for all the residues, consequently producing less internal packing and a variety of water accessible cavities inside and between the protofilaments. Moreover, the consequence of the hydrogen bond-dominated structure might be the unfavorable burial of polar and charged groups in the amyloid structure. In their comprehensive thermodynamic study on polar-apolar mutant proteins, Makhatadze and co-workers (39) described a significant negative contribution of the burial of polar groups to the unfolding ΔC_p. One may speculate that in such a situation, a similar ΔC_p may indicate higher overall burial in the amyloid structure compared with the native, globular state.

ΔH, Suggesting Decreased Internal Packing—There are two main effects responsible for ΔH of protein unfolding: the hydration of the buried groups that become exposed in the unfolded state and the disruption of internal interactions such as van der Waals' interactions, H-bonds, etc. (17, 40, 41). For the thermal unfolding of globular proteins, ΔH, which varies significantly depending on the protein species, increases with an increase in temperature, then it tends to saturate approaching a common ΔH value, independent of protein species, at around 120 °C. Although the temperature-dependent increase of ΔH is caused by the hydration of the buried groups, the unique ΔH value at 120 °C represents the internal interactions common to

various proteins. It was shown that a simple empirical equation is able to quantify the enthalpy of protein unfolding as a function of the changes in the solvent-accessible polar and apolar surface areas and the changes in protonation and in other effects (40). This indicates the structural similarities between different globular proteins: similar atomic compositions, distributions of pairwise interactions, and similar packing densities (40).

ΔH of the dissociation of the amyloid fibrils as normalized per molar monomers proved to be significantly less than that of the unfolding of native β2m (Table I). From the observed similar ΔC_p values, we assumed a similar extent of overall surface burial in the native and amyloid forms, suggesting similar ΔH contributions by the hydration term. Therefore, the observed decrease in ΔH seems to be a result of another term, namely the different internal interactions. It is generally accepted that there is a stronger and more persistent backbone H-bond network in the amyloid structure than in the globular fold of proteins, coupled with the increase in the β-sheet content (32). Although we cannot estimate the enthalpy contribution of H-bonds in the amyloid state for lack of a detailed structure, H-bonds have a positive contribution to ΔH, indicating that we have to search for other oppositely contributing effects to explain the observed smaller ΔH values.

A reasonable explanation of the decreased ΔH is a lower level of side chain packing in the amyloid form. In the amyloid form, the side chain packing cannot be as optimal as in the native state, because the structure is determined by the extensively H-bonded, β-structured backbones. In a systematic study using packing and polar-nonpolar mutants Loladze *et al.* (41) showed that removal of one methylene group from the interior of the protein molecule will destabilize the protein and decrease the enthalpy by 12 kJ/mol through decreased van der Waals' interactions. These interactions are proportional to the square of the packing density (17), which might explain the enthalpy loss of the amyloid form, compared with the native state. Moreover, in the native state of the proteins the unfavorable burial of polar groups is usually compensated by H-bonding (43). It is possible that, in the amyloid form, some polar side chains cannot find H-bonding partners and therefore decrease the stability and enthalpy.

Entropy-driven Free Energy of Fibril Formation—By determining the equilibrium monomer concentration in the fibril solution, we calculated the apparent free energy changes of unfolding or depolymerization (Table I). The $\Delta G_{app} = 43.9$ kJ/mol value at 37 °C is significantly higher than the 19 kJ/mol stability of the native state; the fibril formation is much preferred to the folding to the native state. Consideration of the mixing entropy increases the difference by $RT\ln 55.5$. Although a direct comparison of the two free energy changes may be difficult because of the different types of reactions, we still can assert that the amyloid fibrils exhibit greater stability and that this can only be a result of a more favorable entropy contribution because of the decreased enthalpy term. Compared with the native state, the unfavorable entropy contributions to the amyloid formation are: the decrease in translational/rotational entropy with the decrease in the number of monomeric β2m molecules in the solution and the unfavorable conformational entropy of the H-bonded rigid backbone. These destabilizing effects could be opposed by the increased conformational entropy of the side chains as a result of the lower level of packing and possibly greater surface burial in the amyloid state. As our results reveal, below 13 °C the amyloid formation is purely entropy driven because of the unfavorable ΔH term. A unique theoretical work may provide an explanation describing the amyloid formation by a novel entropy-induced interaction of large "bodies" in a solvent of small molecules (44).

Conclusions—By introducing a novel method, we directly measured the ΔC_p and ΔH of the amyloid formation of β2m by ITC. The observed thermodynamic properties of the amyloid state of β2m go beyond the validity of those empirical functions of globular proteins, revealing a different architecture and energetics of the amyloid structure. The main difference between the native and amyloid form is manifested in the extended β-sheet structure accompanied by a low level of internal packing of the side chains, the possible unfavorable burial of polar and charged groups, and the presence of solvent-accessible cavities in the amyloid fibrils. This image of the amyloid structure is in accordance with pressure studies on transthyretin variants revealing that hydration and packing are crucial to amyloidogenesis (45). This may also explain the fact that, although most of the proteins may be capable of amyloid formation under appropriate extreme conditions, only less than two dozen proteins and peptides cause amyloid diseases.

Acknowledgments—Dr. Kardos thanks F. Vonderviszt and Z. Gugolya (University of Veszprém, Hungary) for help at the beginning of the work and C. Magyar and Z. Dosztányi for molecular graphics.

REFERENCES

1. Rochet, J. C., and Lansbury, P. T., Jr. (2000) *Curr. Opin. Struct. Biol.* **10,** 60–68
2. Sipe, J. D. (1992) *Annu. Rev. Biochem.* **61,** 947–975
3. Gejyo, F., Yamada, T., Odani, S., Nakagawa, Y., Arakawa, M., Kunimoto, T., Kataoka, H., Suzuki, M., Hirasawa, Y., Shirahama, T., Cohen, A. S., and Schmid, K. (1985) *Biochem. Biophys. Res. Commun.* **129,** 701–706
4. Dobson, C. M. (2003) *Nature* **426,** 884–890
5. Stefani, M., and Dobson, C. M. (2003) *J. Mol. Med.* **81,** 678–699
6. Schuler, B., Rachel, R., and Seckler, R. (1999) *J. Biol. Chem.* **274,** 18589–18596
7. Chiti, F., Webster, P., Taddei, N., Clark, A., Stefani, M., Ramponi, G., and Dobson, C. M. (1999) *Proc. Natl. Acad. Sci. U. S. A.* **96,** 3590–3594
8. Sunde, M., Serpell, L. C., Bartlam, M., Fraser, P. E., Pepys, M. B., and Blake, C. C. (1997) *J. Mol. Biol.* **273,** 729–739
9. Sunde, M., and Bake, C. (1997) *Adv. Protein Chem.* **50,** 123–159
10. Antzutkin, O. N., Balbach, J. J., Leapman, R. D., Rizzo, N. W., Reed, J., and Tycko, R. (2000) *Proc. Natl. Acad. Sci. U. S. A.* **97,** 13045–13050
11. Chiti, F., Taddei, N., Stefani, M., Dobson, C. M., and Ramponi, G. (2001) *Protein Sci.* **10,** 879–886
12. Souillac, P. O., Uversky, V. N., Millett, I. S., Khurana, R., Doniach, S., and Fink, A. L. (2002) *J. Biol. Chem.* **277,** 12657–12665
13. Ramirez-Alvarado, M., Merkel, J. S., and Regan, L. (2000) *Proc. Natl. Acad. Sci. U. S. A.* **97,** 8979–8984
14. Taddei, N., Capanni, C., Chiti, F., Stefani, M., Dobson, C. M., and Ramponi, G. (2001) *J. Biol. Chem.* **276,** 37149–37154
15. Chiti, F., Stefani, M., Taddei, N., Ramponi, G., and Dobson, C. M. (2003) *Nature* **424,** 805–808
16. Freire, E. (1995) *Methods Mol. Biol.* **40,** 191–218
17. Makhatadze, G. I., and Privalov, P. L. (1995) *Adv. Protein. Chem.* **47,** 307–425
18. Shnyrov, V. L., Villar, E., Zhadan, G. G., Sanchez-Ruiz, J. M., Quintas, A., Saraiva, M. J., and Brito, R. M. (2000) *Biophys. Chem.* **88,** 61–67
19. Yutani, K., Takayama, G., Goda, S., Yamagata, Y., Maki, S., Namba, K., Tsunasawa, S., and Ogasahara, K. (2000) *Biochemistry* **39,** 2769–2777
20. Martsev, S. P., Dubnovitsky, A. P., Vlasov, A. P., Hoshino, M., Hasegawa, K., Naiki, H., and Goto, Y. (2002) *Biochemistry* **41,** 3389–3395
21. Rezaei, H., Choiset, Y., Eghiaian, F., Treguer, E., Mentre, P., Debey, P., Grosclaude, J., and Haertle, T. (2002) *J. Mol. Biol.* **322,** 799–814
22. Litvinovich, S. V., Brew, S. A., Aota, S., Akiyama, S. K., Haudenschild, C., and Ingham, K. C. (1998) *J. Mol. Biol.* **280,** 245–258
23. Leavitt, S., and Freire, E. (2001) *Curr. Opin. Struct. Biol.* **11,** 560–566
24. Lopez, M. M., and Makhatadze, G. I. (2002) *Methods Mol. Biol.* **173,** 121–126
25. Kim, Y. S., Randolph, T. W., Manning, M. C., Stevens, F. J., and Carpenter, J. F. (2003) *J. Biol. Chem.* **278,** 10842–10850
26. Terzi, E., Holzemann, G., and Seelig, J. (1995) *J. Mol. Biol.* **252,** 633–642
27. Terzi, E., Holzemann, G., and Seelig, J. (1994) *Biochemistry* **33,** 1345–13450
28. Floege, J., and Ketteler, M. (2001) *Kidney Int.* **59,** S164-S171
29. Chiba, T., Hagihara, Y., Higurashi, T., Hasegawa, K., Naiki, H., and Goto, Y. (2003) *J. Biol. Chem.* **278,** 47016–47024
30. Naiki, H., Higuchi, K., Hosokawa, M., and Takeda, T. (1989) *Anal. Biochem.* **177,** 244–249
31. Naiki, H., and Gejyo, F. (1999) *Methods Enzymol.* **309,** 305–318
32. Hoshino, M., Katou, H., Hagihara, Y., Hasegawa, K., Naiki, H., and Goto, Y. (2002) *Nat. Struct. Biol.* **9,** 332–336
33. Naiki, H., Hashimoto, N., Suzuki, S., Kimura, H., Nakakuki, K., and Gejyo, F. (1997) *Amyloid Int. J. Exp. Clin. Invest.* **4,** 223–232
34. Hasegawa, K., Ono, K., Yamada, M., and Naiki, H. (2002) *Biochemistry* **41,** 13489–13498

35. Kozhukh, G. V., Hagihara, Y., Kawakami, T., Hasegawa, K., Naiki, H., and Goto, Y. (2002) *J. Biol. Chem.* **277,** 1310–1315
36. Kad, N. M., Myers, S. L., Smith, D. P., Smith, D. A., Radford, S. E., and Thomson, N. H. (2003) *J. Mol. Biol.* **330,** 785–797
37. Gómez, J., Hilser, V. J., Xie, D., and Freire, E. (1995) *Proteins* **22,** 404–412
38. Katou, H., Kanno, T., Hoshino, M., Hagihara, Y., Tanaka, H., Kawai, T., Hasegawa, K., Naiki, H., and Goto, Y. (2002) *Protein Sci.* **11,** 2218–2229
39. Loladze, V. V., Ermolenko, D. N., and Makhatadze, G. I. (2001) *Protein Sci.* **10,** 1343–1352
40. Hilser, V. J., Gómez, J., and Freire, E. (1996) *Proteins* **26,** 123–133
41. Loladze, V. V., Ermolenko, D. N., and Makhatadze, G. I. (2002) *J. Mol. Biol.* **320,** 343–357
42. Fändrich, M., and Dobson, C. M. (2002) *EMBO J.* **21,** 5682–5690
43. McDonald, I. K., and Thornton, J. M. (1994) *J. Mol. Biol.* **238,** 777–793
44. Kinoshita, M. (2004) *Chem. Phys. Lett.* **387,** 54–60
45. Ferrão-Gonzales, A. D., Palmieri, L., Valory, M., Silva, J. L., Lashuel, H., Kelly, J. W., and Foguel, D. (2003) *J. Mol. Biol.* **328,** 963–974

Direct Measurement of the Thermodynamic Parameters of Amyloid Formation by Isothermal Titration Calorimetry

József Kardos, Kaori Yamamoto, Kazuhiro Hasegawa, Hironobu Naiki and Yuji Goto

J. Biol. Chem. 2004, 279:55308-55314.
doi: 10.1074/jbc.M409677200 originally published online October 19, 2004
